Supplementary Information (SI) for Journal of Analytical Atomic Spectrometry.

Supporting Information

Ion Sampling in ICP-MS: Linking Plasma Expansion, Interface Physics, and Ion Transmission

Hamid Moezzi Rafie, Sina Alavi, Javad Mostaghimi

MECHANICAL & INDUSTRIAL DEPARTMENT, UNIVERSITY OF TORONTO, 5 KING'S COLLEGE ROAD, TORONTO, ONTARIO, M5S 3G8, CANADA

***Corresponding Authors:** salavi@mie.utoronto.ca, mostag@mie.utoronto.ca

Table of Contents:

S1. Langmuir Probe Methodology

A Langmuir probe is a diagnostic tool used to determine key plasma parameters by inserting a small, biased electrode directly into the plasma and recording the resulting current–voltage (I–V) characteristic (Figure S1). As the probe bias is swept from large negative to large positive voltages relative to the plasma potential, three distinct regions appear in the I–V curve (Figure S2). In the ion-saturation region, at sufficiently negative bias, nearly all collected charge is due to ions, and the current plateaus at the ion-saturation current, $I_{i,sat}$. As the bias moves toward the floating potential V_f (where the net current is zero), the transition region (or electron-retarding region) exhibits an exponential rise in electron current I_e; plotting $\ln(I_e)$ versus voltage in this regime yields a straight line whose slope is proportional to $1/T_e$, where T_e is the electron temperature. Finally, in the electron-saturation region, at high positive bias, electrons dominate the collected current and I_e again levels off at the electron-saturation current $I_{e,sat}$.

Figure S1.. Designed Langmuir probe.

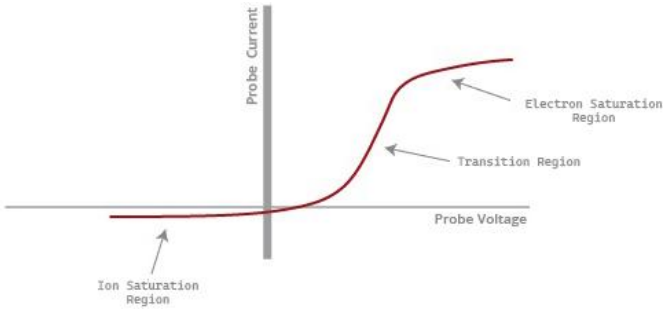

Figure S2. A characteristic I-V curve obtained from Langmuir probe measurements.

From these regions, plasma properties are extracted using orbital-motion-limited (OML) theory for a cylindrical probe.[11] The electron temperature is determined by fitting the slope of the semi-log plot in the transition region:

$$ln(I_e) \propto \frac{e(V - V_f)}{k_B T_e}$$

Where e is the electron charge, V is the voltage, and k_B is the Boltzmann constant. Once T_e is known, the absolute level of $I_{e,sat}$ is used to calculate electron density via:

$$I_e = e n_e A \sqrt{\frac{k_B T_e}{2\pi m_e}}$$

Where n_e is electron number density, A is the probe collection area and m_e the electron mass. Together, these measurements provide a localized “snapshot” of plasma conditions, making the Langmuir probe an indispensable tool for characterizing ion sampling regions in ICP-MS interfaces.

In our experiments, Langmuir probe measurements were carried out with the tungsten-rod probe positioned 7 mm downstream of the sampling orifice, inserted coaxially through the aluminum flange and Swagelok seal described earlier. Outside the chamber, the probe electrode was connected in series with a resistor (Figure S3) and to a DC power supply, while the voltage drops across the resistor and the probe bias voltage were recorded concurrently on a dual-channel oscilloscope (Figure S4). A

voltage sweep from –90 V to +90 V was applied to the probe, and the resultant current was computed from the measured resistor voltage drop via Ohm's law. The resulting I–V characteristic was then plotted, and key parameters, floating potential, electron temperature and number density were extracted from the graphs obtained through a developed MATLAB code.

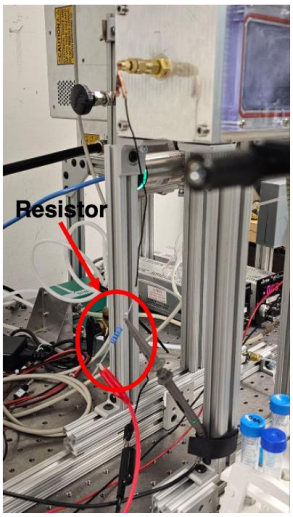

Figure S3. The known resistor connected in series with the tungsten rod.

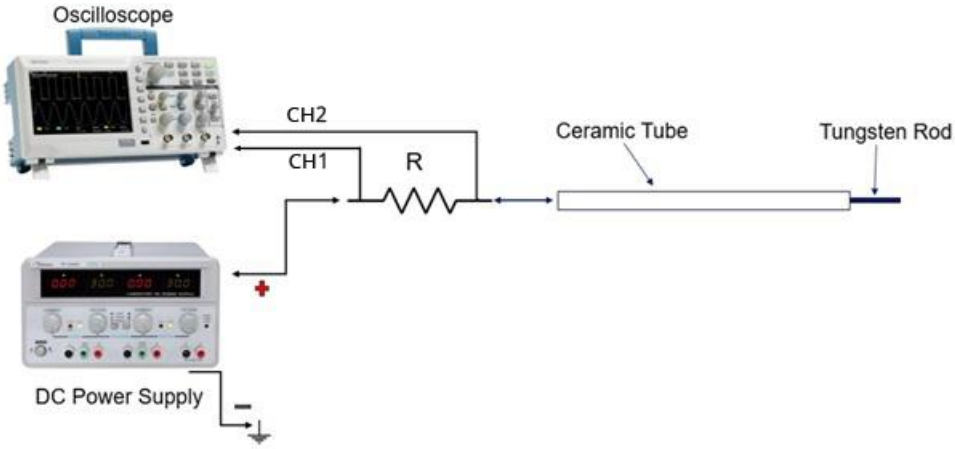

Figure S4. Langmuir Probe circuit.

S2: Image Processing Methodology

Figure S5. shows the mirror installed inside the vacuum chamber to better visualize the shock structure:

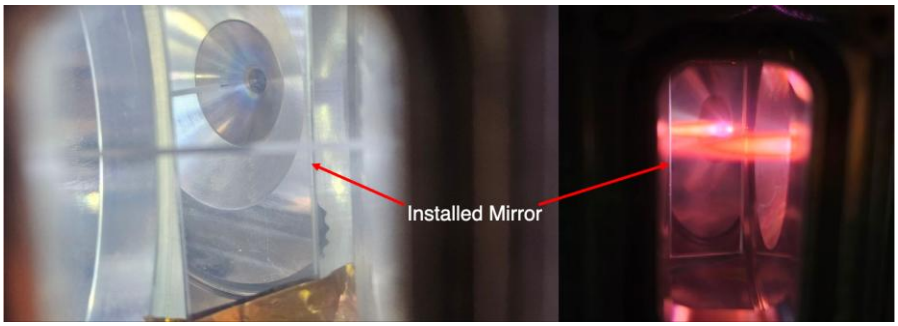

Figure S5. Installed mirror inside the vacuum chamber.

All shock-structure images were loaded into MATLAB and converted to grayscale to simplify intensity analysis. According to Figure S6, the brightest pixel, corresponding to the sampling-orifice exit, was identified as the origin, and a line was traced from that point along the centerline. Light intensities along this line were then plotted against pixel position, and the pixel scale was converted to millimeters using the known sampling cone dimensions. Any subsequent local maxima downstream of the origin in the intensity profile were taken as the Mach disk locations.

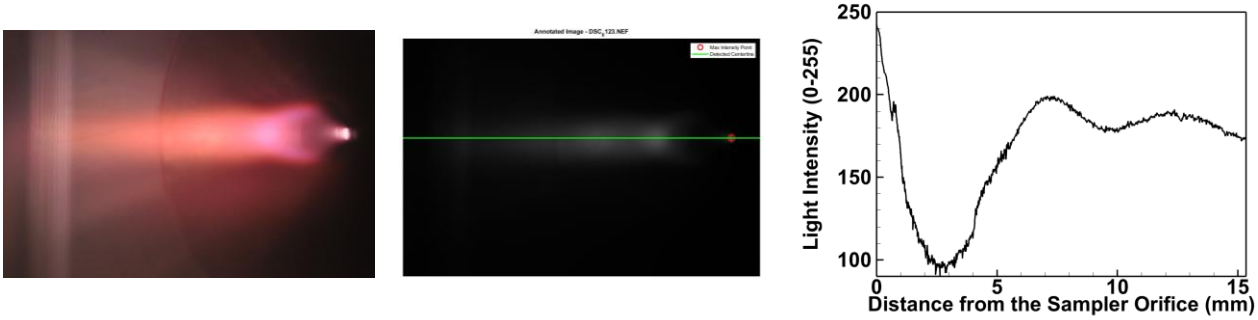

Figure S6. MATLAB image processing workflow.

S3. Supersonic Jet Images:

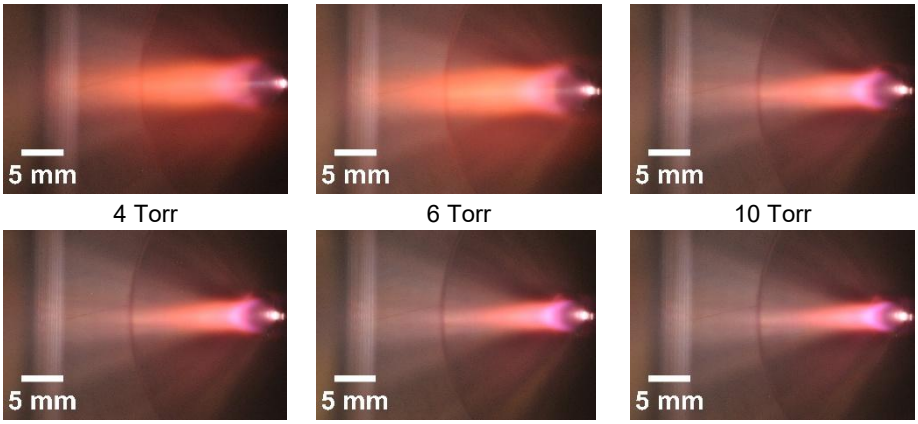

Figure S7. Images of the supersonic jet at various vacuum pressures for a 0.8 mm diameter sampling orifice at 900 W and 0.6 L/min injector gas flowrate.

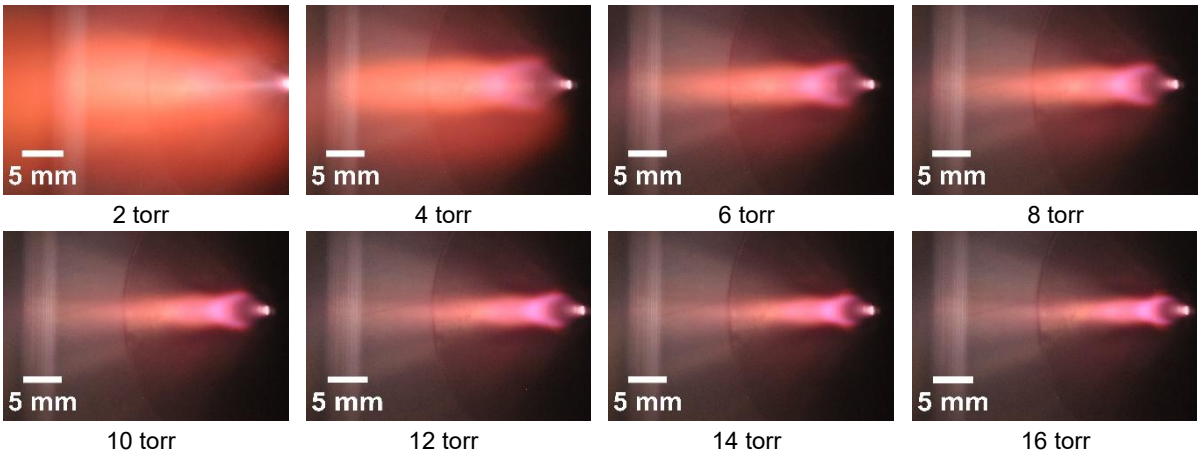

Figure S8. Images of the supersonic jet at various vacuum pressures for a 1 mm diameter sampling orifice at 900 W and 0.6 L/min injector gas flowrate.

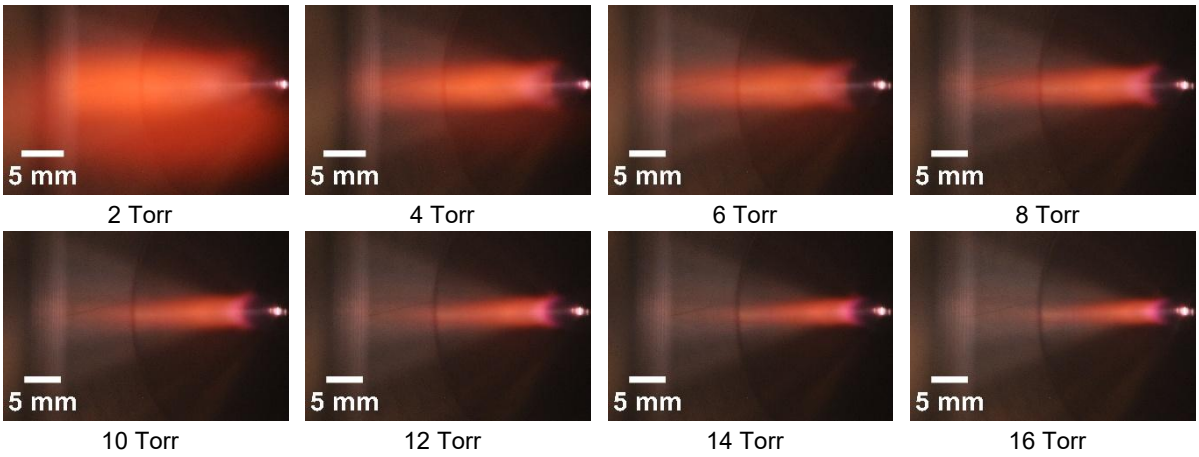

Figure S9. Images of the supersonic jet at various vacuum pressures for a 0.8 mm diameter sampling orifice at 700 W and 0.6 L/min injector gas flowrate.

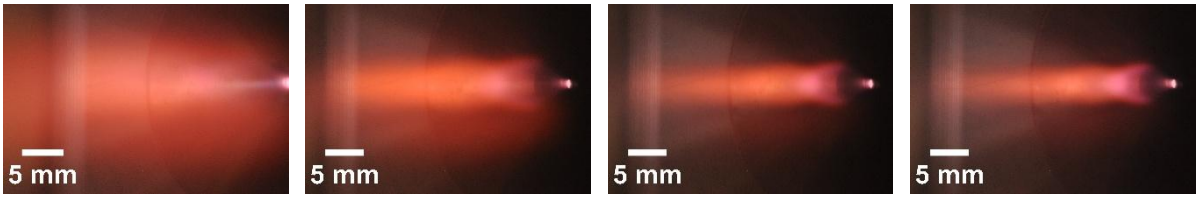

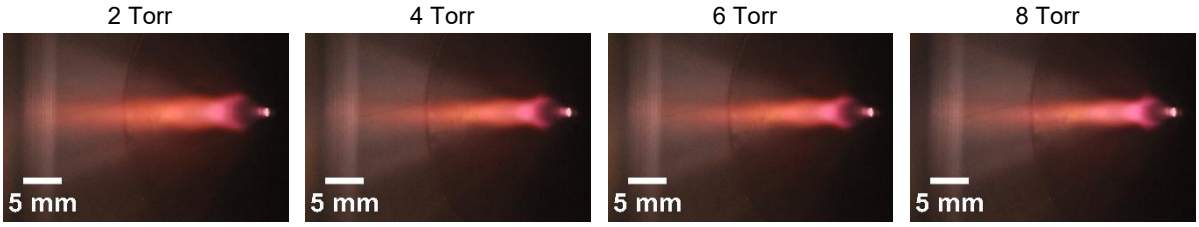

Figure S10. Images of the supersonic jet at various vacuum pressures for a 1 mm diameter sampling orifice at 700 W and 0.6 L/min injector gas flowrate.

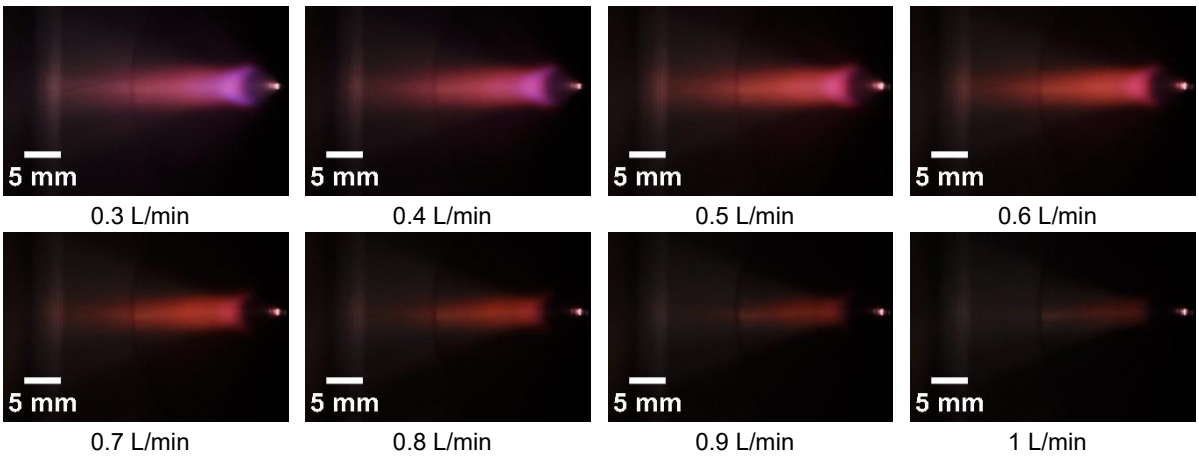

Figure S11. Images of the supersonic jet for various injector gas flowrates at a vacuum pressure of 8 torr, a sampling orifice diameter of 0.8 mm and a RF Power of 900 W.

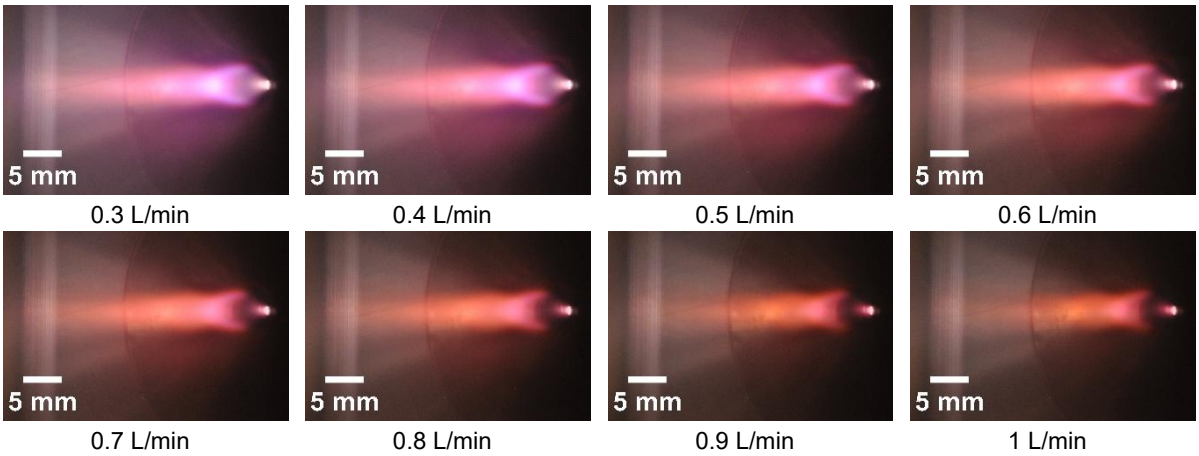

Figure S12. Images of the supersonic jet for various injector gas flowrates at a vacuum pressure of 8 torr, a sampling orifice diameter of 1 mm and a RF Power of 900 W.

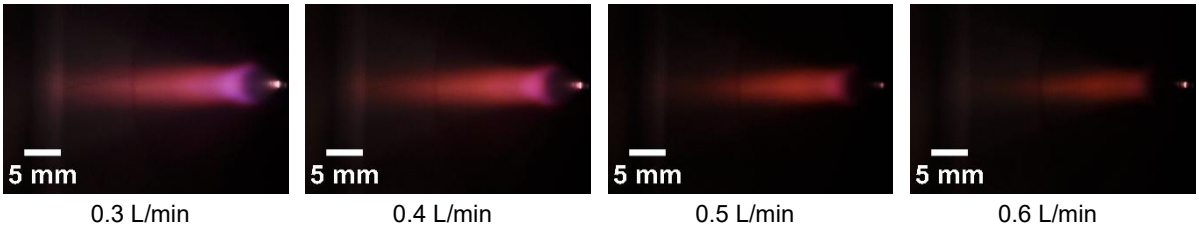

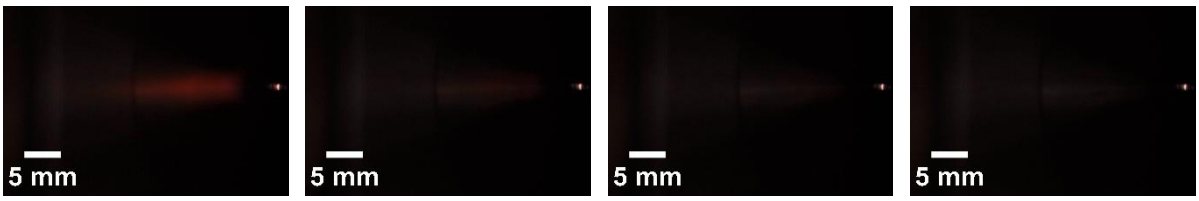

0.7 L/min 0.8 L/min 0.9 L/min 1 L/min

Figure S13. Images of the supersonic jet for various injector gas flowrates at a vacuum pressure of 8 torr, a sampling orifice diameter of 0.8 mm and a RF Power of 700 W.

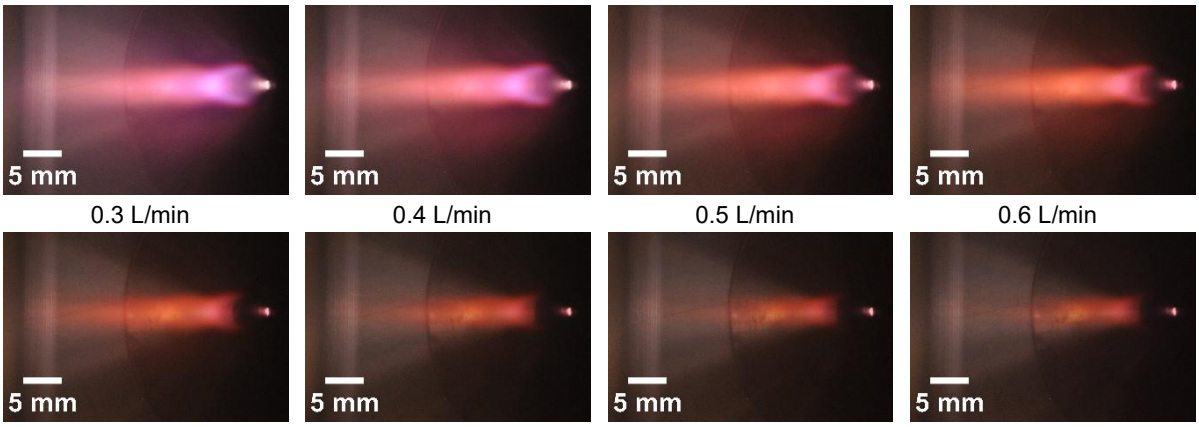

0.3 L/min 0.4 L/min 0.5 L/min 0.6 L/min

0.7 L/min 0.8 L/min 0.9 L/min 1 L/min

Figure S14. Images of the supersonic jet for various injector gas flowrates at a vacuum pressure of 8 torr, a sampling orifice diameter of 1 mm and a RF Power of 700 W.